Supporting Information for

Autocatalytic Surface Reduction and Its Role in Controlling Seed-Mediated Growth of Colloidal Metal Nanocrystals

Tung-Han Yang,[a,b] Shan Zhou,[c] Kyle D. Gilroy,[a] Legna Figueroa-Cosme,[c] Yi-Hsien Lee,[b] Jenn-Ming Wu,[b] and Younan Xia*[,a,c,d]

[a]The Wallace H. Coulter Department of Biomedical Engineering, Georgia Institute of Technology and Emory University, Atlanta, Georgia 30332, United States

[b]Department of Materials Science and Engineering, National Tsing Hua University, Hsinchu, 30013, Taiwan

[c]School of Chemistry and Biochemistry, Georgia Institute of Technology, Atlanta, Georgia 30332, United States

[d]School of Chemical and Biomolecular Engineering, Georgia Institute of Technology, Atlanta, Georgia 30332, United States

*Corresponding author. E-mail: younan.xia@bme.gatech.edu

This Supporting Information file includes:

Materials and Methods, Tables S1 to S5, Figures S1 to S18, and References

Materials and Methods

Chemicals. Sodium tetrachloropalladate (Na_2PdCl_4), potassium tetrabromopalladate (K_2PdBr_4), L–ascorbic acid (AA), citric acid (CA), poly(vinyl pyrrolidone) (PVP, $M_W \approx 55{,}000$), formaldehyde (HCHO), sodium borohydride ($NaBH_4$), sodium sulfate (Na_2SO_4), diethylene glycol (DEG), and potassium bromide (KBr) were all obtained from Sigma–Aldrich. Ethylene glycol (EG) was purchased from J. T. Baker. Deionized (DI) water with a resistivity of 18.2 MΩ·cm was used for all the experiments.

Quantitative analysis of reduction kinetics of $PdBr_4^{2-}$-based precursor in the presence of seeds. We measured the reduction rates by analyzing the concentration of Pd(II) ions remaining in the reaction solution at different time points using UV−vis spectroscopy. In the standard procedure, 7.8 mL of an aqueous solution containing 60 mg of AA (a reductant) and 100 mg of PVP (a colloidal stabilizer) was mixed with 0.2 mL of the seeds (0.36 mg) in a 20-mL glass vial at a specific temperature of 0, 10, 22, and 30 °C for 30 min under magnetic stirring. Next, 2.0 mL of an aqueous solution containing 1.71 mg of K_2PdBr_4 was quickly added in one shot. Meanwhile, the timer started running. An aliquot of 0.2 mL was sampled from the reaction solution at each time point and immediately injected into 0.8 mL of highly concentrated KBr (500 mg/mL) aqueous solution held at 0 °C to quench the reduction and thus preserve the concentration of Pd(II) ions. Additionally, the hydrolysis of $PdBr_4^{2-}$ also could be suppressed by using highly concentrated KBr aqueous solution, enabling the precise determination of the Pd(II) precursor concentrations by UV-vis analyses.[1,2] In the quenched solution, the Pd(II) precursor should mainly exist in the form of $PdBr_4^{2-}$. The quenched solution was then centrifuged at 55000 rpm for 60 min to precipitate out all the Pd nanocrystals, leaving behind $PdBr_4^{2-}$ ions in the supernatant for UV–vis measurement (using the absorption of $PdBr_4^{2-}$ peaked at 332 nm). The centrifuge used was the Beckman Coulter

Optima MAX-XP ultracentrifuge, with a TLA-55 rotor. The time–dependent concentrations of $PdBr_4^{2-}$ ions remaining in the solution could be derived by comparing the obtained UV–vis spectrum with the calibration curve derived from the $PdBr_4^{2-}$ solutions. The calibration curve provided in Fig. S6 *A* and *B* was obtained from stock solutions prepared by adding different amounts of Na_2PdCl_4 into 1 mL of an aqueous solution containing 400 mg of KBr, 2 mg of PVP, and 1.2 mg of AA. The same aqueous KBr solution was also used to quench the reduction involved in a synthesis prior to UV-vis measurement. Due to the involvement of an excess amount of KBr, the $PdCl_4^{2-}$ ions were supposed to be completely converted to $PdBr_4^{2-}$ through ligand exchange.

Synthesis of Pd nanocubes (7, 12, and 18 nm) to be used as the seeds. The Pd nanocubes with different edge lengths of 7, 12, 18 nm were synthesized using the previously reported protocols with minor modifications.[3,4] Typically, 8 mL aqueous solution containing PVP (105 mg), AA (60 mg), and different amounts of KBr and KCl were added into a 20 mL vial. The solution was pre-heated at 80 °C for 5 min before the addition of 3 mL Na_2PdCl_4 aqueous solution (64.6 mM). The addition of KBr and KCl in the following amounts gave the nanocubes with edge lengths of 7 nm (75 mg of KBr and 141 mg of KCl), 12 nm (300 mg of KBr), and 18 nm (600 mg of KBr), respectively. The reaction was then capped, and maintained at 80 °C for 3 h under magnetic stirring. After centrifugation and washing with water three times, the Pd nanocubes were dispersed in water for further use.

Synthesis of Pd nanocubes (23 nm) to be used as the seeds. 8 mL aqueous solution containing PVP (105 mg), AA (60 mg), and KBr (1200 mg) were placed in a 20 mL vial, and pre-heated in air under magnetic stirring at 80 °C for 5 min. Then, 3.0 mL of an aqueous solution containing Na_2PdCl_4 (57 mg) was added in one shot using a pipette. The reaction was then capped, and the reaction was allowed to proceed at 80 °C for 3 h under magnetic stirring. After 3 h, 4 mL

aqueous solution containing PVP (52.5 mg) and AA (30 mg) were immediately added into the reaction solution, and maintained at 80 °C for 5 min. Then, 1 mL of Na_2PdCl_4 aqueous solution (19 mg) was injected into the reaction solution at a rate of 1 mL/h using a syringe pump at 80 °C. After the addition of Na_2PdCl_4, the solution was maintained with magnetic stirring for 10 min to allow the reaction to complete. After centrifugation and washing with water three times, the Pd nanocubes were dispersed in water for further use.

Synthesis of Pd polyhedra with different proportions of {100} to {111} facets to be used as the seeds. The Pd cuboctahedra, truncated octahedra, and octahedra were prepared by following our previous protocols.[5] Typically, 0.3 mL of an aqueous suspension of the 12-nm Pd nanocubes (1.8 mg/mL in concentration) and 8 mL of an aqueous solution containing HCHO (100 μL) and PVP (105 mg) were added into a 20-mL vial, which had been heated at 60 °C for 10 min under magnetic stirring. Afterwards, 3 mL of aqueous solution containing Na_2PdCl_4 was introduced in one shot. The addition of Na_2PdCl_4 in the following amounts gave cuboctahedra (8.7 mg), truncated octahedra (17.4 mg), and octahedra (29.0 mg), respectively. Each reaction was allowed to proceed at 60 °C for 3 h under magnetic stirring. After centrifugation and washing with water four times, the final products were dispersed in water for further use.

Preparation of capping-free Pd seeds. The capping-free Pd seeds were prepared by directly removing the surface-chemisorbed Br^- ions from the as-grown Pd nanocubes (Figs. 1*A* and S14 *A-C*), cuboctahedra (Fig. S11*A*), truncated octahedra (Fig. S11*B*), and octahedra (Fig. 1*B*) by subjecting the sample to a mild reductive condition according to our previous report with minor modifications.[4] Typically, 3 mL of an aqueous suspension of the Pd seeds (1.8 mg/mL) and 10 mL of EG containing 100 mg of PVP and 100 mg of CA were mixed in a 20-mL vial. The mixture

was hosted in a vial and then capped and aged at 120 °C for 18 h. After centrifuging at 17500 rpm and washing with ethanol once and water three times, the products were dispersed in 3 mL of water.

Synthesis of Pd decahedra (19 nm) to be used as the seeds. The Pd decahedral seeds with the size of 19 nm (Fig. 4*A*) were synthesized using a previously reported protocol with modifications.[6] Typically, 160 mg PVP and 174 mg Na_2SO_4 were dissolved in 8 mL DEG (hosted in a 20-mL vial), and then heated at 105 °C for 5 min. At the same time, 62 mg Na_2PdCl_4 was dissolved in 4 mL DEG and the solution was injected in one shot into the pre-heated solution. The reaction was maintained at 105 °C for 3 h under magnetic stirring. The product was collected by centrifugation, washed once with acetone and twice with water and finally dispersed in water for further use.

Synthesis of Pd icosahedra (12 nm) to be used as the seeds. The Pd icosahedral seeds with the size of 12 nm (Fig. 4*B*) were synthesized using a previously reported protocol.[7] Typically, 80 mg PVP was dissolved in 2 mL DEG (hosted in a 20-mL vial), and then heated at 130 °C for 10 min. At the same time, 15.5 mg Na_2PdCl_4 was dissolved in 1 mL DEG and the solution was injected in one shot to the pre-heated solution. The reaction was maintained at 130 °C for 3 h under magnetic stirring. The product was collected by centrifugation, washed once with acetone and twice with water and finally dispersed in water for further use.

Characterizations. Transmission electron microscopy (TEM) images were taken using a Hitachi HT7700 microscope operated at 120 kV. The samples for TEM analysis were prepared by drop casting the nanoparticles dispersions on carbon-coated Cu grids and then drying them under ambient conditions. UV–vis absorption spectra were measured using a Perkin–Elmer Lambda 750 UV–vis–NIR spectrometer.

Calculation of the ratio between the numbers of Br^- ions and surface Pd{100} atoms.

Case #1: Pd cubic seeds.

In a previous report,[4] it was confirmed that the chemisorption of Br^- ions only occurred on Pd{100} rather than Pd{111} facets. Based on this finding, we expect that the Br^- ions released from the Pd(II) precursor should mainly adsorb to the {100} facets of Pd cubic seeds in the present study. Under this approximation, based on the ratio of Br^- ions to all Pd atoms (a value of 1.50×10^{-2}) obtained from ICP-MS analysis, the ratio between the number of Br^- ions and surface Pd{100} atoms after the seed-mediated growth (Fig. 1*E*) was calculated using the equation:

$$\frac{Br^- \, ions}{surface \, Pd(100) \, atoms} = \frac{\frac{Br^- \, ions}{total \, Pd \, atoms} * number \, of \, Pd \, atoms \, per \, cube}{number \, of \, Pd \, atoms \, on \, Pd(100) \, surface \, per \, cube}$$

$$= \frac{\frac{Br^- \, ions}{total \, Pd \, atoms} * 4 * \left(\frac{l^3}{a^3}\right)}{6 * 2 * \left(\frac{l^2}{a^2}\right)} = \frac{\frac{Br^- \, ions}{total \, Pd \, atoms} * \frac{l}{a}}{3} \qquad \text{(Eq. S1)}$$

where l is the average edge length of {100} facets on the Pd nanocubes (20.7 nm, Fig. 1*E*); a is the lattice constant of Pd (0.389 nm). Note that we assumed a perfect cubic shape for the Pd nanocrystals after the growth for the estimation of the number of Pd atoms per cube in this case (Fig. 1*E*). According to Eq. S1, the ratio between the numbers of Br^- ions and surface Pd{100} atoms after the growth of cubic seeds was estimated to be 0.27.

Case #2: Pd octahedral seeds.

The ratio of Br^- ions to all Pd atoms (a value of 8.12×10^{-3}) was obtained from ICP-MS analysis. The ratio between the number of Br^- ions and surface Pd{100} atoms after the seed-

mediated growth (Fig. 1*F*) was calculated according to the equation:

$$\frac{Br^- \, ions}{surface \, Pd(100) \, atoms}$$

$$= \frac{\frac{Br^- \, ions}{total \, Pd \, atoms} * number \, of \, Pd \, atoms \, per \, runcated \, octahedron}{number \, of \, Pd \, atoms \, on \, Pd(100) \, surface \, per \, truncated \, octahedron}$$

$$= \frac{\frac{Br^- \, ions}{total \, Pd \, atoms} * 4 * \left(\frac{8 * \sqrt{2} * l^3}{a^3}\right)}{6 * 2 * \left(\frac{l^2}{a^2}\right)}$$

$$= \frac{\frac{Br^- \, ions}{total \, Pd \, atoms} * 8 * \sqrt{2} * \frac{l}{a}}{3} \qquad \text{(Eq. S2)}$$

where l is the average edge length of {100} facets of Pd truncated octahedral nanocrystals (9.8 nm, Fig. 1*F*); and a is the lattice constant of Pd (0.389 nm). Note that we assumed a truncated octahedral shape for the Pd nanocrystals after the seed-mediated growth. This allows us to estimate the number of Pd atoms per truncated octahedron (Fig. 1*F*). According to Eq. S2, the ratio between the number of Br^- ions and surface Pd{100} atoms for the octahedral seed after the synthesis was estimated to be 0.77.

Determination of the rate constants for solution reduction (k_1) and surface reduction (k_2) of precursor in the absence of Pd seed based on the Finke–Watzky model.[2,8] In the absence of preformed seeds, the reduction of the Pd(II) can be described using the following steps:

$$\mathrm{Pd(II)} + 2e^- \xrightarrow{k_1} \mathrm{Pd^0} \qquad \text{(Eq. S3)}$$

(solution reduction)

$$n\mathrm{Pd}^0 \xrightarrow{homogeneous\ nucleation} \mathrm{Pd}_n^0 \qquad \text{(Eq. S4)}$$

(homogeneous nucleation of the just-formed atoms to form nuclei)

$$\mathrm{Pd}_n^0 + \mathrm{Pd(II)} + 2e^- \xrightarrow{k_2} \mathrm{Pd}_{n+1}^0 \qquad \text{(Eq. S5)}$$

(autocatalytic surface reduction on the just-formed nuclei)

where Pd(II) represents the precursor, Pd^0 is the just-formed atom, and Pd_n^0 are the surface atoms on the just-formed nuclei. Due to the high energy of zero-valent Pd atoms generated from the solution reduction of Pd(II), it is expected that the homogeneous nucleation of the just-formed Pd atoms would take place at an extremely fast rate compared to the rate of the precursor reduction while causing no change to the concentration of Pd(II). Thus, the homogeneous nucleation step can be excluded when we consider the reduction rate of Pd(II). The overall reduction rate for Pd(II) can be expressed as[2,8]

$$\frac{-\mathrm{d[Pd(II)]}}{\mathrm{d}t} = k_1[\mathrm{Pd(II)}] + k_2[\mathrm{Pd(II)}][\mathrm{Pd}_n^0] \qquad \text{(Eq. S6)}$$

By substituting for $[\mathrm{Pd}_n^0] = [\mathrm{Pd(II)}]_0 - [\mathrm{Pd(II)}]$, we obtain the following equation, which can be integrated and then evaluated at the indicated limits:

$$\frac{-\mathrm{d[Pd(II)]}}{\mathrm{d}t} = k_1[\mathrm{Pd(II)}] + k_2[\mathrm{Pd(II)}]([\mathrm{Pd(II)}]_0 - [\mathrm{Pd(II)}])$$

$$\int_{[\mathrm{Pd(II)}]_0}^{[\mathrm{Pd(II)}]} \frac{-\mathrm{d}[\mathrm{Pd(II)}]}{[\mathrm{Pd(II)}](k_1 + k_2([\mathrm{Pd(II)}]_0 - [\mathrm{Pd(II)}]))} = \int_0^t \mathrm{d}t$$

$$\ln\left[\frac{(k_1 + k_2([\mathrm{Pd(II)}]_0 - [\mathrm{Pd(II)}]))[\mathrm{Pd(II)}]_0}{k_1[\mathrm{Pd(II)}]}\right] = (k_1 + k_2[\mathrm{Pd(II)}]_0) * t$$

Expressing the resultant equation (above) in the exponential format:

$$[\mathrm{Pd(II)}]_t = \frac{\frac{k_1}{k_2} + [\mathrm{Pd(II)}]_0}{1 + \frac{k_1}{k_2[\mathrm{Pd(II)}]_0} * \exp((k_1 + k_2[\mathrm{Pd(II)}]_0) * t)} \quad \text{(Eq. S7)}$$

Determination of the rate constants for surface reduction (k_2') of precursor in the presence of Pd seeds. Due to the lack of *in-situ* characterization tools that can directly observe the growth of nanocrystals with a satisfied resolution, it is impossible to calculate the concentrations of surface Pd atoms, $\mathrm{Pd}_n^0(\mathrm{seed})$, on the growing seeds at different stages of a synthesis. In the present work, we assume that the surface area of preformed seeds is constant during the growth since the size of preformed seeds after growth is not changed significantly. For example, the size of the Pd cubic seeds, assuming a perfect cubic shape during growth, slightly increased from 18.0 ± 2.1 nm to 20.7 ± 2.4 nm after 4 h when $PdBr_4^{2-}$ was added as the precursor (Fig. 1 *A* and *E*). The concentration of surface Pd atoms of the resultant 20.7 ± 2.4-nm Pd cubes was estimated to be 0.0389 mM. According to the calculation, the concentration of surface Pd atoms on the seeds increased by 32% after the growth. Overall, the assumption of constant surface area of preformed seeds during the growth introduces a certain error, but it should be still within the acceptable range since the average size of preformed seeds after growth is not changed dramatically. Moreover, in the present study, the surface reduction on the nucleus can be excluded since all of the newly

formed Pd atoms are deposited onto the performed seeds and thus homogeneous nucleation is suppressed (Figs. 1, 4, S11 and S14) under these experimental conditions.

In the presence of preformed seeds, we have:

$$\mathrm{Pd(II)} + 2e^- \xrightarrow{k_1} \mathrm{Pd^0} \qquad \text{(Eq. S8)}$$

(solution reduction)

$$\mathrm{Pd^0} + \mathrm{Pd_n^0(seed)} \xrightarrow{heterogeneous\ nucleation} \mathrm{Pd_{n+1}^0(seed)} \qquad \text{(Eq. S9)}$$

(heterogeneous nucleation of the just-formed atoms on the performed seeds)

$$\mathrm{Pd_n^0(seed)} + \mathrm{Pd(II)} + 2e^- \xrightarrow{k_2'} \mathrm{Pd_{n+1}^0(seed)} \qquad \text{(Eq. S10)}$$

(autocatalytic surface reduction on the performed seeds)

where $\mathrm{Pd_n^0(seed)}$ are the surface atoms on the performed seeds. Due to the high energy of zero-valent Pd atoms, it is expected that heterogeneous nucleation of the just-formed Pd atoms on the performed seeds would take place at an extremely fast rate compared to the rate of precursor reduction. As such, the heterogeneous nucleation of the just-formed Pd atoms on the performed seeds can be excluded when we consider the reduction rate of the precursor. The overall rate for the reduction of Pd(II) precursor can be expressed as

$$\frac{-\mathrm{d[Pd(II)]}}{\mathrm{d}t} = k_1[\mathrm{Pd(II)}] + k_2'[\mathrm{Pd(II)}][\mathrm{Pd_n^0(seed)}] \qquad \text{(Eq. S11)}$$

where $[Pd_n^0(seed)]$ represents the concentration of surface atoms on the performed seeds introduced into the reaction solution.

$$\frac{-d[Pd(II)]}{dt} = [Pd(II)](k_1 + k_2'[Pd_n^0(seed)])$$

$$\frac{1}{k_1 + k_2'[Pd_n^0(seed)]} * \int_{[Pd(II)]_0}^{[Pd(II)]} \frac{-d[Pd(II)]}{[Pd(II)]} = \int_0^t dt$$

$$\ln\left[\frac{[Pd(II)]}{[Pd(II)]_0}\right] = -(k_1 + k_2'[Pd_n^0(seed)]) * t$$

Expressing the resultant equation (above) in the exponential format (Eq. S12):

$$[Pd(II)]_t = [Pd(II)]_0 * \exp(-(k_1 + k_2'[Pd_n^0(seed)]) * t) \qquad \text{(Eq. S12)}$$

The rate constant (k_1) can be determined by fitting the concentration of the precursor in the absence of preformed seeds to the Finke–Watzky model.[2,8] By constraining k_1 to the just obtained value, we are able to quantitatively account for the autocatalytic surface reduction of Pd precursor on the performed seeds through curve fitting (Eq. S12) by obtaining the value of k_2'.

Table S1. Kinetic parameters for the reduction of the Pd(II) precursor in the absence of preformed seeds at different temperatures. Note that the reduction of this precursor was nearly suppressed at 0 °C in the absence of seeds (see Fig. S7*A*).

Temperature	Rate constant	
(°C)	Solution reduction	Surface reduction
0	$k_1 = 0$	$k_2 = 0$
10	$k_1 = 9.10\times10^{-5}$ min^{-1}	$k_2 = 1.61\times10^{-2}$ mM^{-1} min^{-1}
22	$k_1 = 9.17\times10^{-4}$ min^{-1}	$k_2 = 3.53\times10^{-2}$ mM^{-1} min^{-1}
30	$k_1 = 2.80\times10^{-3}$ min^{-1}	$k_2 = 5.80\times10^{-1}$ mM^{-1} min^{-1}

Table S2. Kinetic parameters for the reduction of the Pd(II) precursor in the presence of preformed Pd cubic (18 nm) or octahedral (25 nm) seeds at different temperatures.

Type of seed	Temperature	Rate constant	
	(°C)	Solution reduction	Surface reduction
Cubic	0	$k_1 = 0$	$k_2' = 7.50\times10^{-2}$ mM^{-1} min^{-1}
	10	$k_1 = 9.10\times10^{-5}$ min^{-1}	$k_2' = 1.32\times10^{-1}$ mM^{-1} min^{-1}
	22	$k_1 = 9.17\times10^{-4}$ min^{-1}	$k_2' = 2.61\times10^{-1}$ mM^{-1} min^{-1}
	30	$k_1 = 2.80\times10^{-3}$ min^{-1}	$k_2' = 3.83\times10^{-1}$ mM^{-1} min^{-1}
Octahedral	0	$k_1 = 0$	$k_2' = 1.60\times10^{-2}$ mM^{-1} min^{-1}
	10	$k_1 = 9.10\times10^{-5}$ min^{-1}	$k_2' = 4.42\times10^{-2}$ mM^{-1} min^{-1}
	22	$k_1 = 9.17\times10^{-4}$ min^{-1}	$k_2' = 1.35\times10^{-1}$ mM^{-1} min^{-1}
	30	$k_1 = 2.80\times10^{-3}$ min^{-1}	$k_2' = 2.74\times10^{-1}$ mM^{-1} min^{-1}

Table S3. Kinetic parameters for the reduction of the Pd(II) precursor in the presence of preformed Pd cubic seeds with different sizes at different temperatures.

Size of seed (nm)	Temperature (°C)	Rate constant	
		Solution reduction	**Surface reduction**
7	0	$k_1 = 0$	$k_2' = 8.80\times10^{-2}$ mM^{-1} min^{-1}
	10	$k_1 = 9.10\times10^{-5}$ min^{-1}	$k_2' = 1.45\times10^{-1}$ mM^{-1} min^{-1}
	22	$k_1 = 9.17\times10^{-4}$ min^{-1}	$k_2' = 2.71\times10^{-1}$ mM^{-1} min^{-1}
	30	$k_1 = 2.80\times10^{-3}$ min^{-1}	$k_2' = 4.08\times10^{-1}$ mM^{-1} min^{-1}
12	0	$k_1 = 0$	$k_2' = 8.20\times10^{-2}$ mM^{-1} min^{-1}
	10	$k_1 = 9.10\times10^{-5}$ min^{-1}	$k_2' = 1.39\times10^{-1}$ mM^{-1} min^{-1}
	22	$k_1 = 9.17\times10^{-4}$ min^{-1}	$k_2' = 2.65\times10^{-1}$ mM^{-1} min^{-1}
	30	$k_1 = 2.80\times10^{-3}$ min^{-1}	$k_2' = 3.99\times10^{-1}$ mM^{-1} min^{-1}
18	0	$k_1 = 0$	$k_2' = 7.50\times10^{-2}$ mM^{-1} min^{-1}
	10	$k_1 = 9.10\times10^{-5}$ min^{-1}	$k_2' = 1.32\times10^{-1}$ mM^{-1} min^{-1}
	22	$k_1 = 9.17\times10^{-4}$ min^{-1}	$k_2' = 2.61\times10^{-1}$ mM^{-1} min^{-1}
	30	$k_1 = 2.80\times10^{-3}$ min^{-1}	$k_2' = 3.83\times10^{-1}$ mM^{-1} min^{-1}
23	0	$k_1 = 0$	$k_2' = 7.21\times10^{-2}$ mM^{-1} min^{-1}
	10	$k_1 = 9.10\times10^{-5}$ min^{-1}	$k_2' = 1.24\times10^{-1}$ mM^{-1} min^{-1}
	22	$k_1 = 9.17\times10^{-4}$ min^{-1}	$k_2' = 2.58\times10^{-1}$ mM^{-1} min^{-1}
	30	$k_1 = 2.80\times10^{-3}$ min^{-1}	$k_2' = 3.72\times10^{-1}$ mM^{-1} min^{-1}

Table S4. Kinetic parameters for the reduction of the Pd(II) precursor in the presence of preformed Pd decahedral or icosahedral seeds at different temperatures.

Type of seed	Temperature (°C)	Rate constant	
		Solution reduction	Surface reduction
Decahedral	0	$k_1 = 0$	$k_2' = 1.93\times10^{-1}$ mM^{-1} min^{-1}
	10	$k_1 = 9.10\times10^{-5}$ min^{-1}	$k_2' = 2.90\times10^{-1}$ mM^{-1} min^{-1}
	22	$k_1 = 9.17\times10^{-4}$ min^{-1}	$k_2' = 4.66\times10^{-1}$ mM^{-1} min^{-1}
	30	$k_1 = 2.80\times10^{-3}$ min^{-1}	$k_2' = 5.82\times10^{-1}$ mM^{-1} min^{-1}
Icosahedral	0	$k_1 = 0$	$k_2' = 2.58\times10^{-1}$ mM^{-1} min^{-1}
	10	$k_1 = 9.10\times10^{-5}$ min^{-1}	$k_2' = 3.73\times10^{-1}$ mM^{-1} min^{-1}
	22	$k_1 = 9.17\times10^{-4}$ min^{-1}	$k_2' = 5.16\times10^{-1}$ mM^{-1} min^{-1}
	30	$k_1 = 2.80\times10^{-3}$ min^{-1}	$k_2' = 6.50\times10^{-1}$ mM^{-1} min^{-1}

Table S5. The concentrations of surface atoms of various types of seeds used in this work.

Type of seed	Size of seed (nm)	Amount of seeds (mg)	Concentration of surface atoms (mM)
Cubic	7	0.36	0.0563
	12	0.36	0.0329
	18	0.36	0.0219
	23	0.36	0.0169
Octahedral	25	0.36	0.0225
Decahedral	19	0.36	0.0381
Icosahedral	12	0.36	0.0472

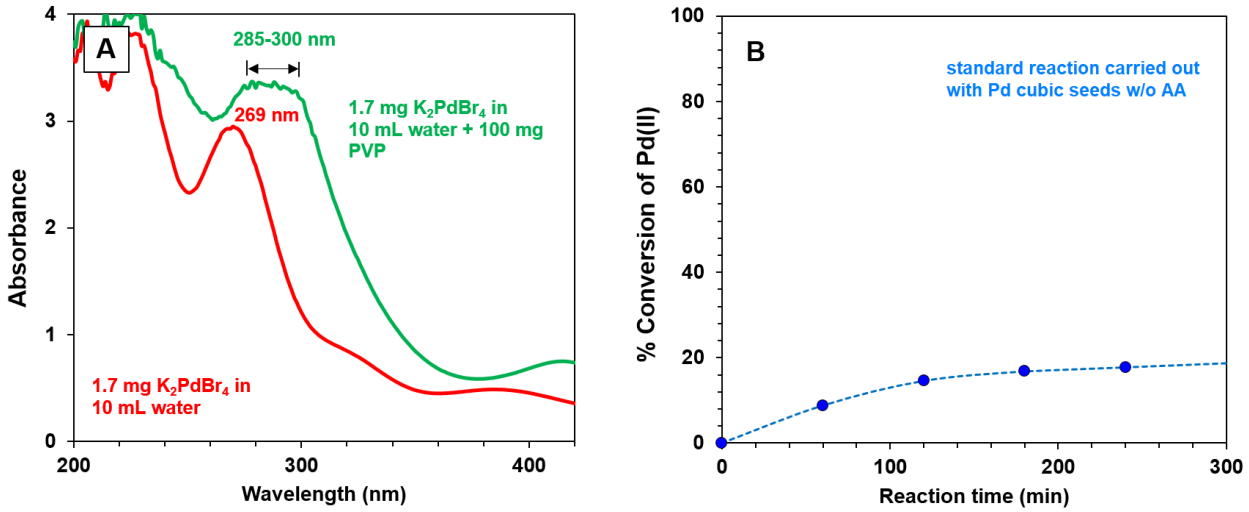

Fig. S1. (A) UV−vis spectra recorded from the freshly prepared aqueous solutions identical to the reaction mixture involved in the standard protocol for seed-mediated growth except for the absence of AA and PVP (red) and the absence of AA only (green). It should be noted that the addition of PVP caused the peak to increase in intensity beyond the detection limit, but clearly presents a shift into the 285–300 nm region. (B) Plot trending the percent conversion of Pd(II) as a function of reaction time in the absence of AA from a standard reaction mixture, revealing that only 13% of the Pd(II) precursor was reduced to Pd atoms within 100 min at 22 °C. In contrast, when AA was present, the percent conversion of the Pd(II) precursor to Pd atoms was nearly 50% after 100 min (Fig. S8*C*).

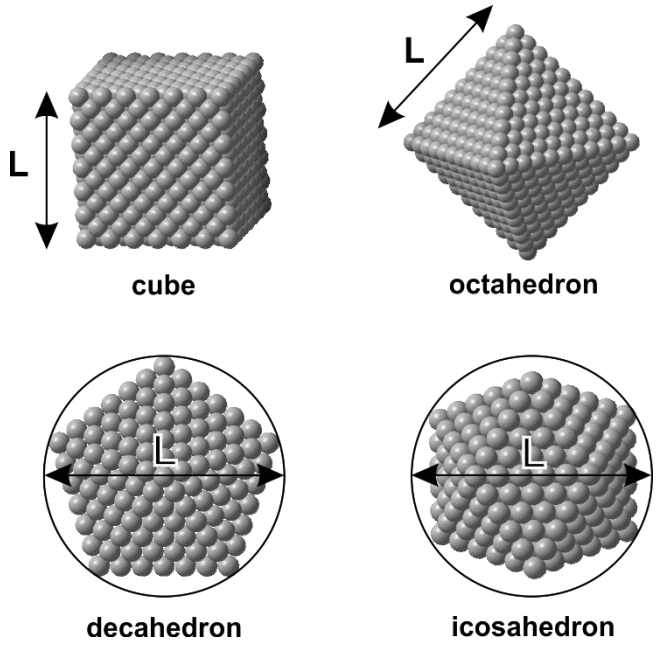

Fig. S2. Schematic illustrations showing how particle size (L) was defined for a cube, octahedron, decahedron, and icosahedron.

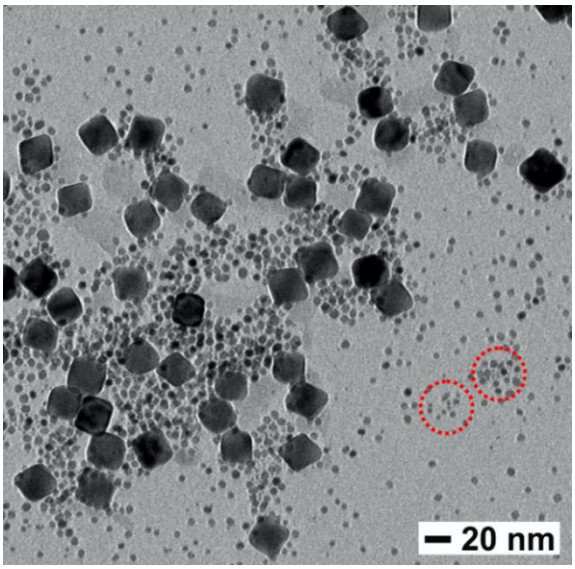

Fig. S3. TEM image of products obtained when $PdCl_4^{2-}$ was added as a precursor in the presence of Pd octahedral seeds using the standard growth procedures. The overgrowth on the octahedral seeds was insignificant. Instead, numerous tiny particles marked by red circles were formed through homogeneous nucleation. It is well documented in literature that Cl^- ions cannot serve an effective capping agent for the Pd surface in the synthesis of Pd nanocrystals.[9] As a result, we rule out the possibility that the Cl^- ions released from $PdCl_4^{2-}$ precursor would affect the growth of Pd nanocrystals under the experimental conditions used in the present study.

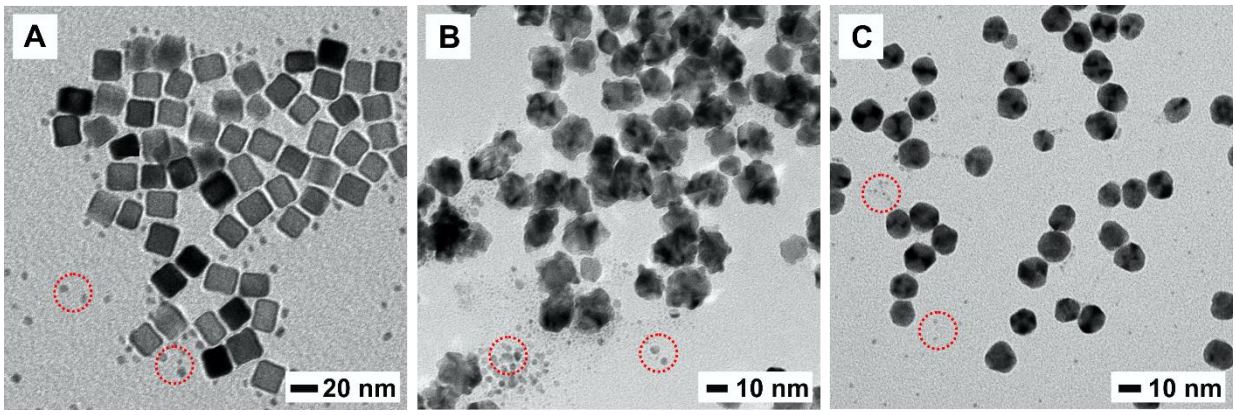

Fig. S4. TEM images of products obtained when $PdCl_4^{2-}$ was added as a precursor in the presence of Pd (*A*) cubic, (*B*) decahedral or (*C*) icosahedral seeds using the standard growth procedure. It is clear that overgrowth occurred on these seeds, but most importantly, numerous tiny particles marked by red circles were formed through homogeneous nucleation. These observations suggest that the reduction of a Pd(II) precursor based on $PdCl_4^{2-}$ mainly underwent solution reduction in which the precursor was reduced to atoms in the solution phase prior to their aggregation into tiny particles through homogeneous nucleation and then growth.

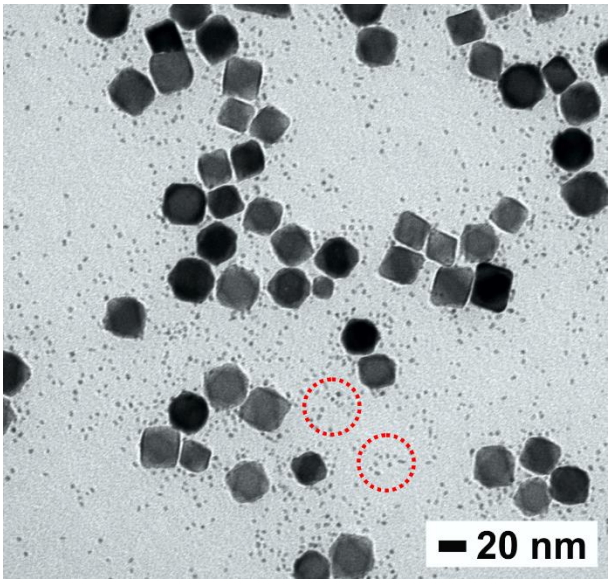

Fig. S5. TEM image of products obtained when the Pd(II) precursor was used in the presence of Pd octahedral seeds, $NaBH_4$, and PVP. In this control experiment, we switched to a much stronger reducing agent (*i.e.*, $NaBH_4$) relative to AA to examine whether the type of reducing agent would affect the reduction pathways (solution reduction *vs.* surface reduction). As shown by the image, overgrowth on the octahedral seeds was insignificant. Instead, there were a lot of particles smaller than the original seeds, implying the presence of homogeneous nucleation. This result suggests that solution reduction dominated over surface reduction when $NaBH_4$ was used as the reducing agent, which is opposite to what was observed in the case of AA (Figs. 1 and 2). It is clear that the reduction pathway of the precursor could be switched between surface and solution by varying the experimental parameters such as the type of reducing agent to alter the reduction kinetics.

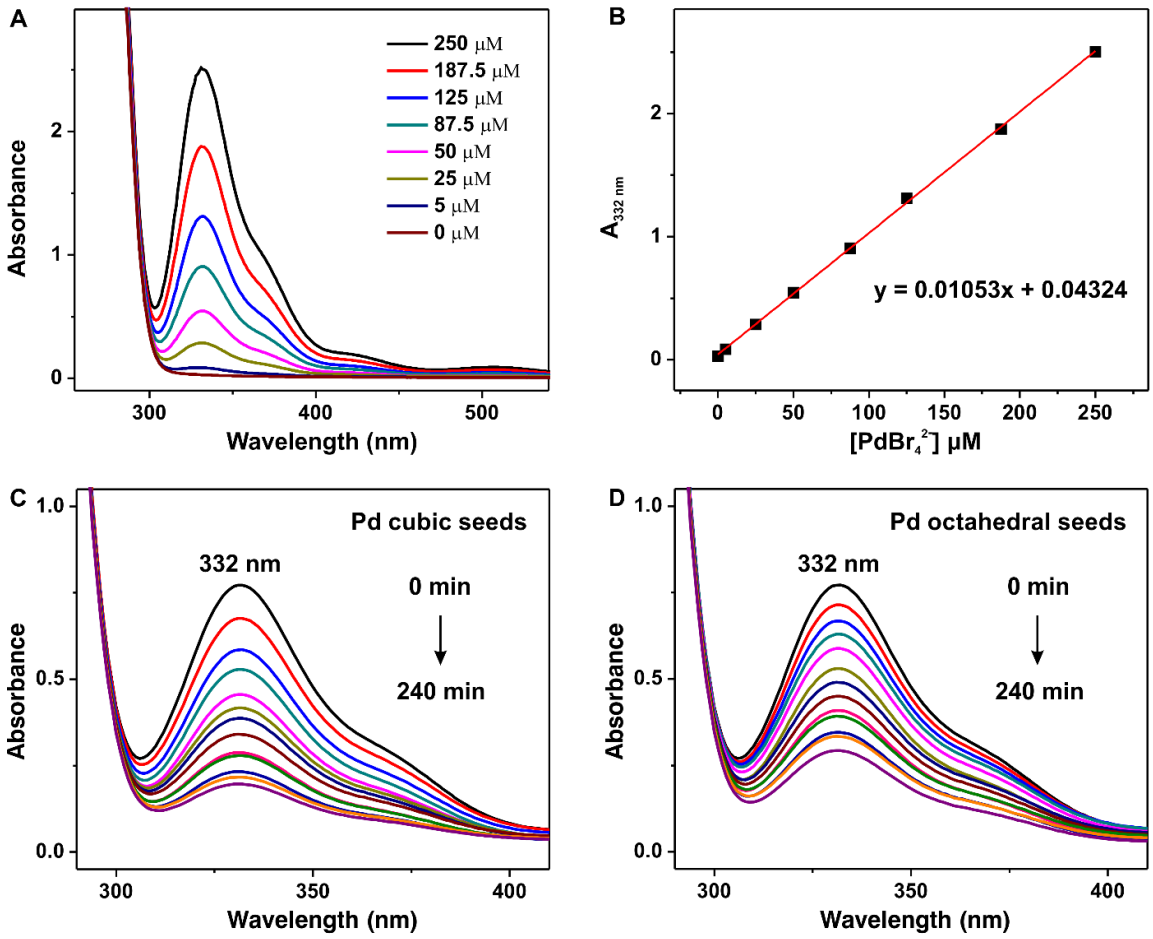

Fig. S6. (*A*) UV−vis spectra of $PdBr_4^{2-}$ stock solutions prepared with different concentrations. The $PdBr_4^{2-}$ stock solutions were prepared by dissolving different amounts of Na_2PdCl_4 in water containing AA, PVP, and KBr.[2] Note that the $PdCl_4^{2-}$ species should be immediately converted to $PdBr_4^{2-}$ through ligand exchange, as confirmed by the position the absorption peak (at 332 nm). (*B*) Plot showing the absorbance at 332 nm as a function of the concentration of $PdBr_4^{2-}$. This calibration curve can be used to determine the concentration of $PdBr_4^{2-}$ remaining in the reaction solution from the UV-vis spectrum of the sample, after the reduction has been quenched with a concentrated KBr solution. (*C*, *D*) UV−vis spectra of the reaction solutions after the Pd(II) precursor has been used in the presence of Pd (*C*) cubic or (*D*) octahedral seeds. The reduction in the sampled aliquot was quenched with a concentrated KBr solution held at 0 °C.

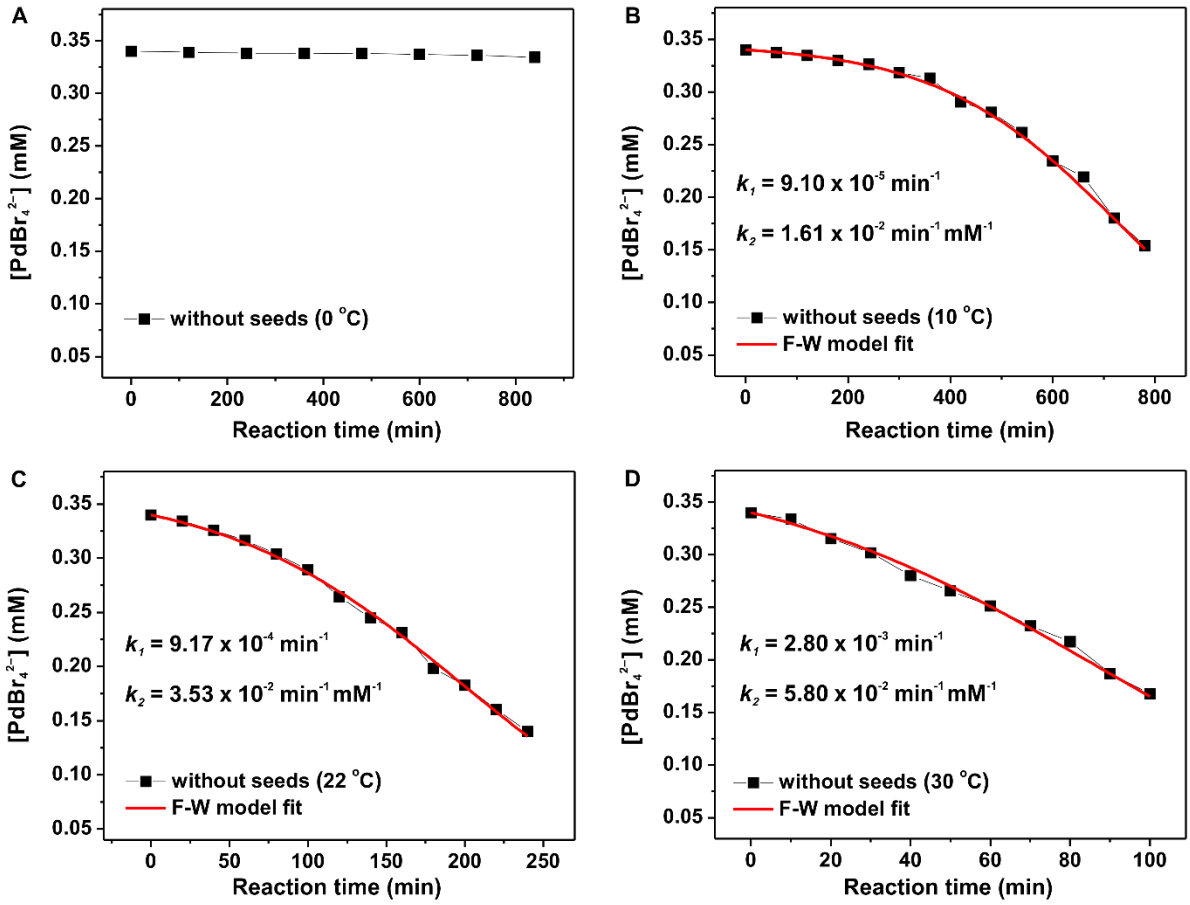

Fig. S7. Plots showing the concentrations of the Pd(II) precursor remaining in the reaction solutions in the absence of seeds when the syntheses were conducted at (*A*) 0, (*B*) 10, (*C*) 22, and (*D*) 30 °C. Note that the reduction was nearly suppressed at 0 °C in the absence of seeds. (*B*-*D*) The experimental data were then fitted using the Finke−Watzky (F−W) model (Eq. S7).[2,8]

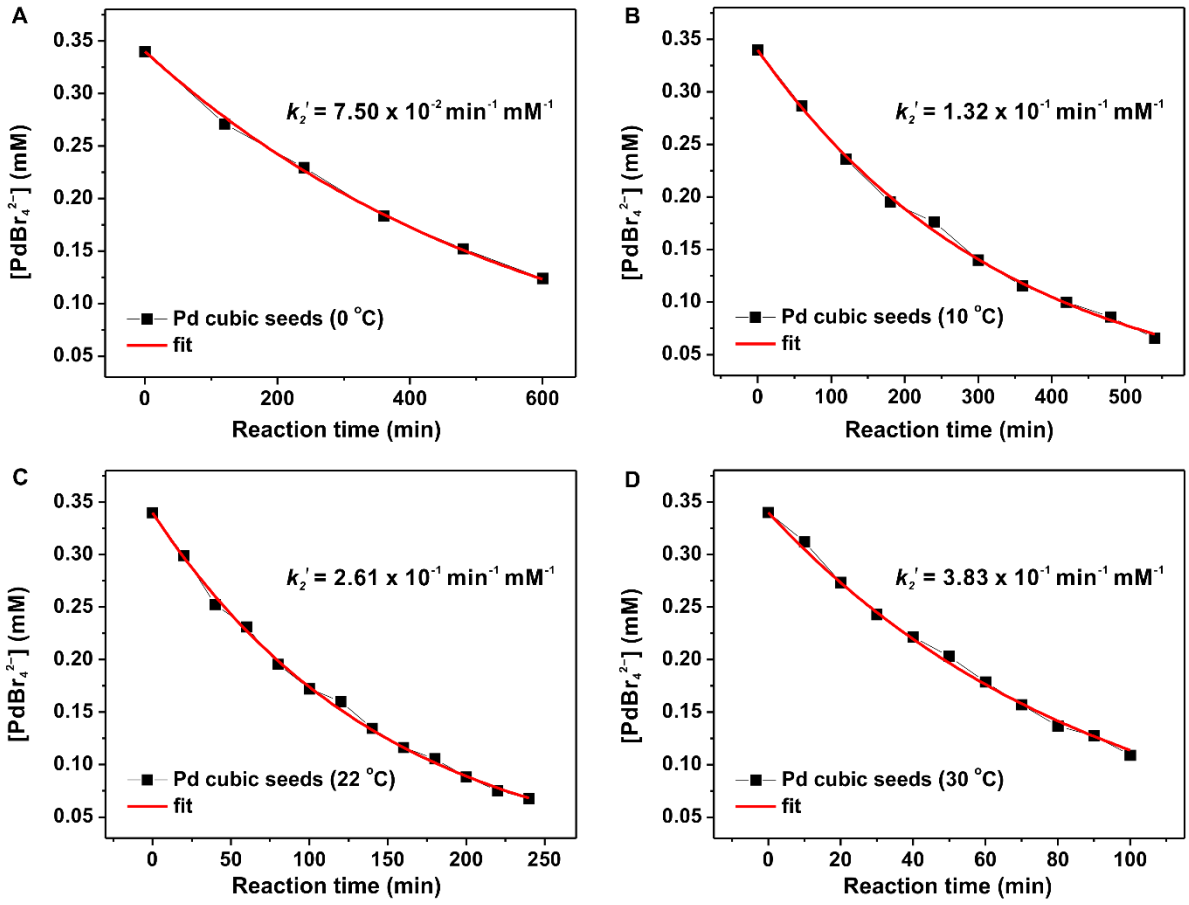

Fig. S8. Plots showing the concentrations of the Pd(II) precursor remaining in the reaction solutions in the presence of Pd cubic seeds when the syntheses were conducted at (*A*) 0, (*B*) 10, (*C*) 22, (*D*) and 30 °C. The experimental data were then fitted using Eq. S12.

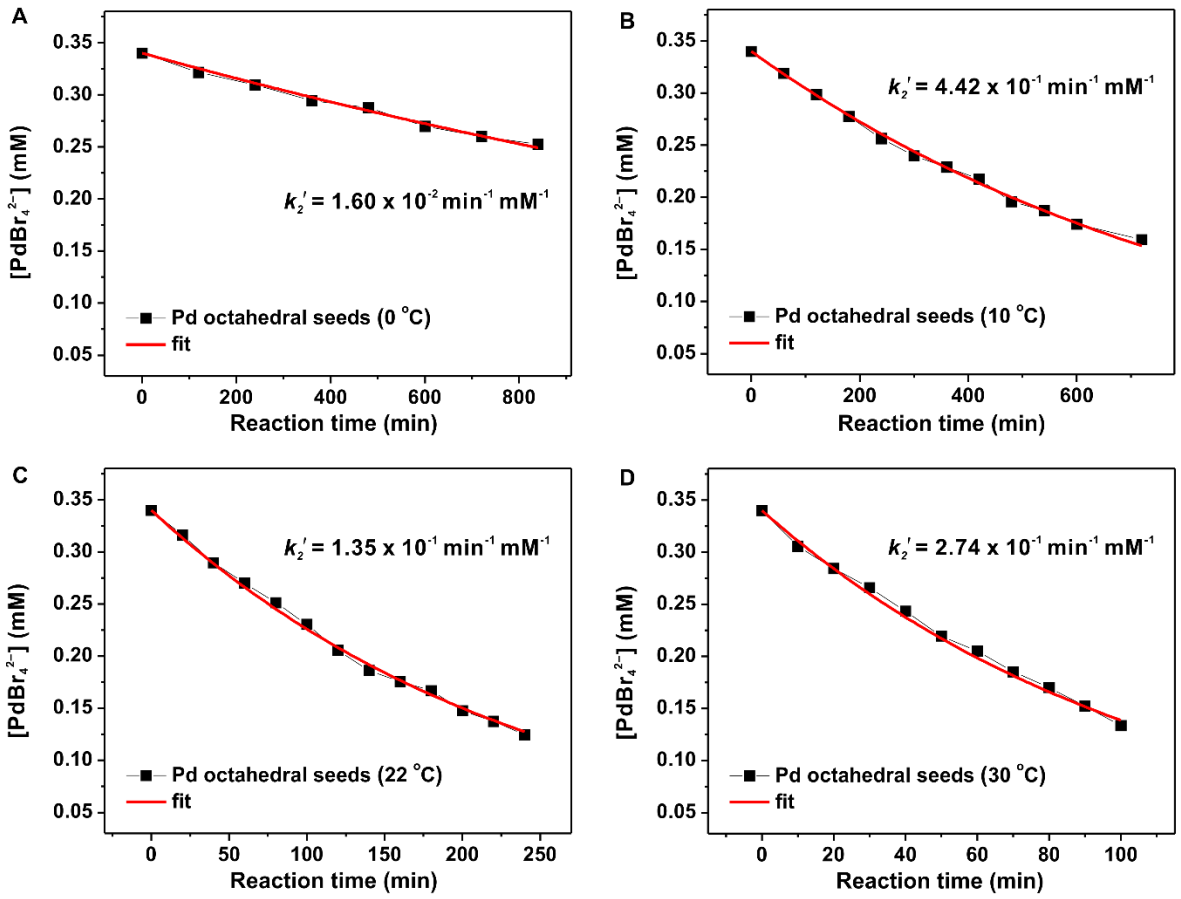

Fig. S9. Plots showing the concentrations of the Pd(II) precursor remaining in the reaction solutions in the presence of Pd octahedral seeds when the syntheses were conducted at (*A*) 0, (*B*) 10, (*C*) 22, (*D*) and 30 °C. The experimental data were then fitted using Eq. S12.

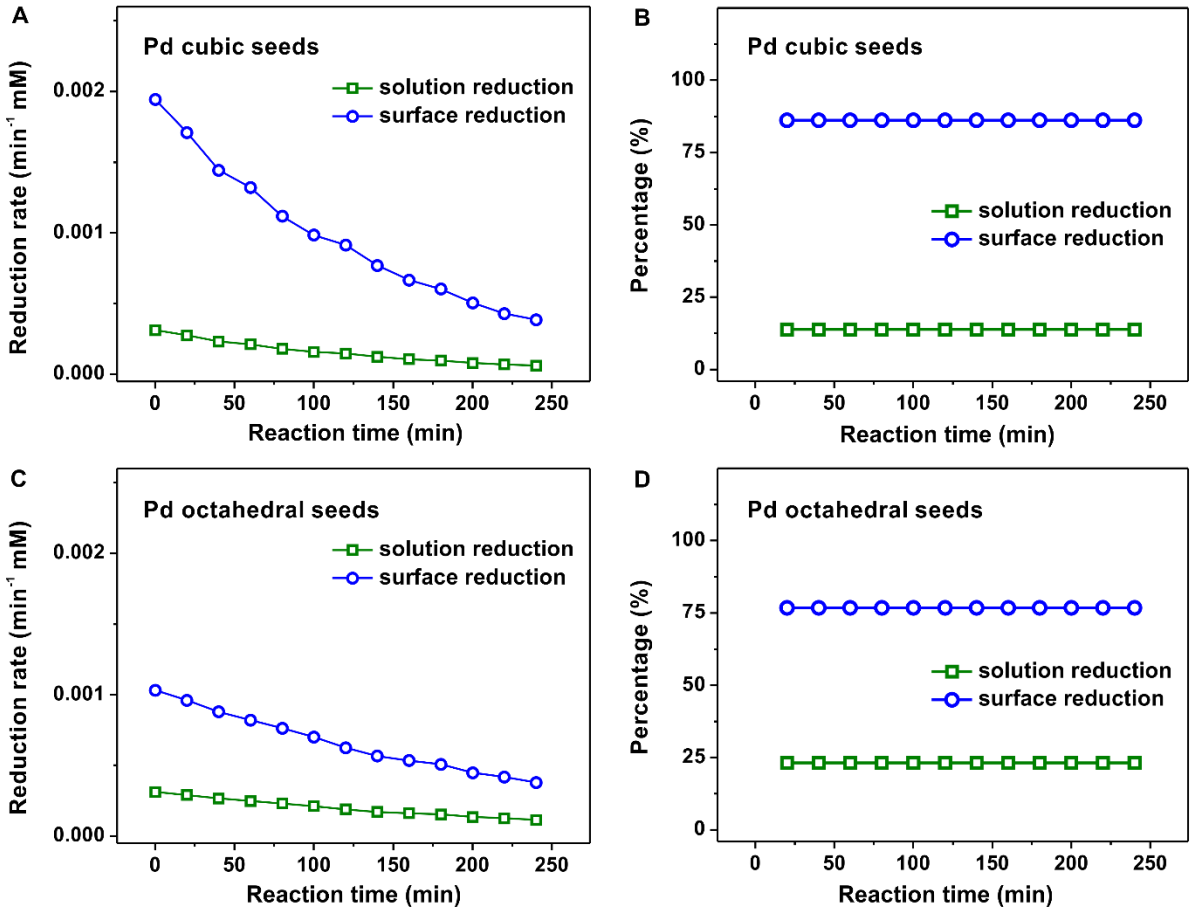

Fig. S10. (*A*, *C*) The rates of solution reduction and surface reduction for the Pd(II) precursor as a function of reaction time in the presence of Pd (*A*) cubic or (*C*) octahedral seeds at 22 °C. (*B*, *D*) The percentages of solution reduction and surface reduction for the Pd(II) precursor as a function of reaction time in the presence of Pd (*B*) cubic or (*D*) octahedral seeds at 22 °C.

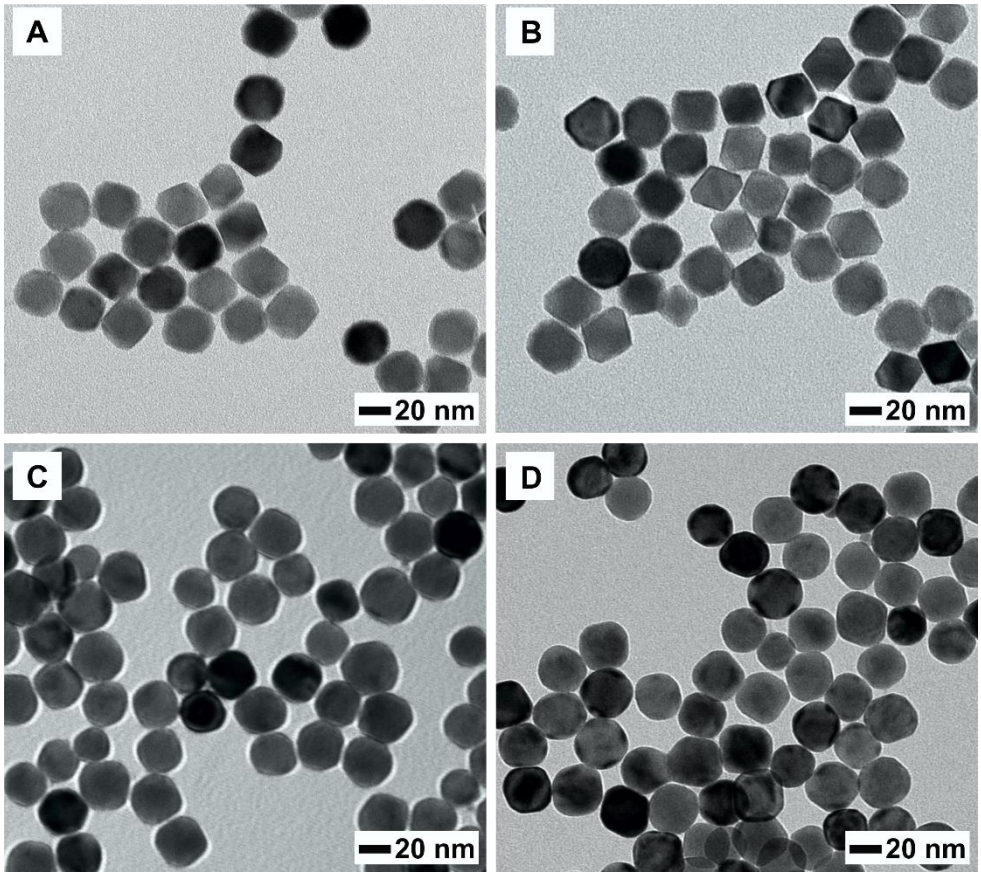

Fig. S11. (*A, C*) TEM images of (*A*) the Pd cuboctahedral seeds and (*C*) the products obtained using the standard growth procedure. (*B, D*) TEM images of (*B*) Pd truncated octahedral seeds and (*D*) the products obtained using the standard growth procedure. Note that the proportion of {100} to {111} for the Pd cuboctahedral seeds is higher than that of truncated octahedral seeds.[5]

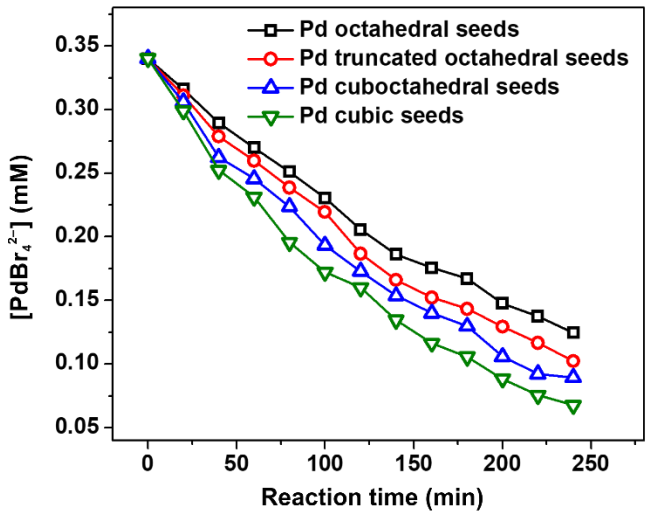

Fig. S12. The concentrations of the Pd(II) precursor remaining in the reaction solutions as a function of time in the presence of Pd cubic (Fig. 2*A*), cuboctahedral, truncated octahedral, or octahedral seeds (Fig. 2*A*) at room temperature. We found that the reduction rate of the Pd(II) precursor followed the trend of cube > cuboctahedron > truncated octahedron > octahedron. This trend suggests that the Pd(II) precursor tended to be reduced to Pd atoms on the {100} facets with a smaller activation energy relative to the {111} facets, which is consistent with the corresponding activation energies obtained from the quantitative measurements in the current study (Fig. 2*B*).

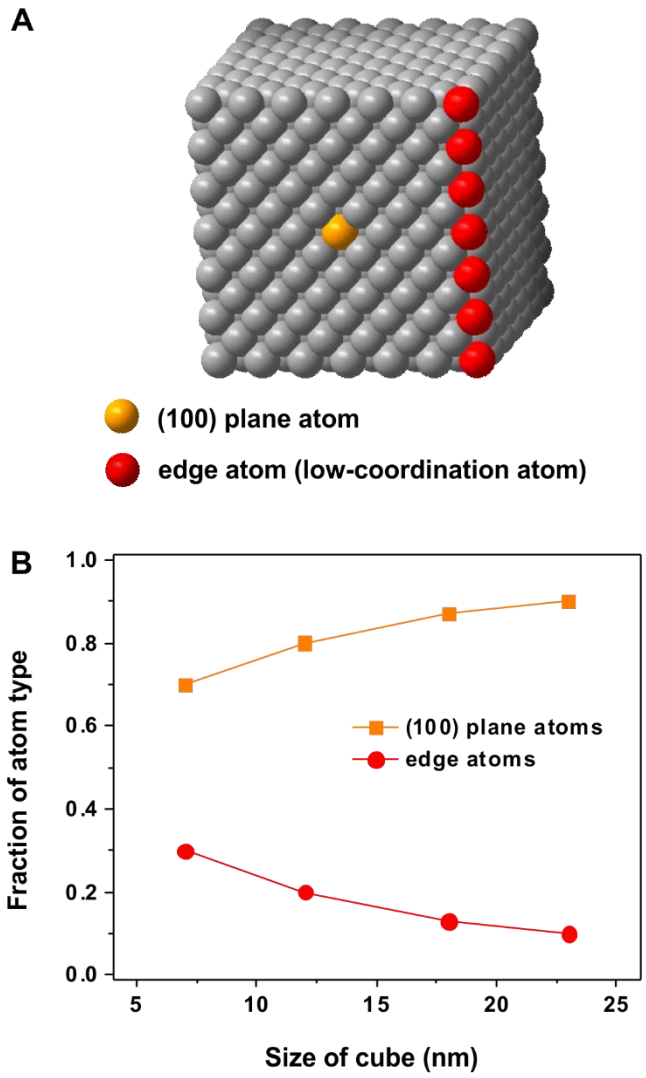

Fig. S13. (*A*) Schematic illustrations of the two types of surface atoms (plane and edge atoms) on a Pd cubic seed. (*B*) Plot trending the fraction of plane and edge atoms versus the size (edge length) of the Pd cubic seeds, taken from reported calculations.[10,11]

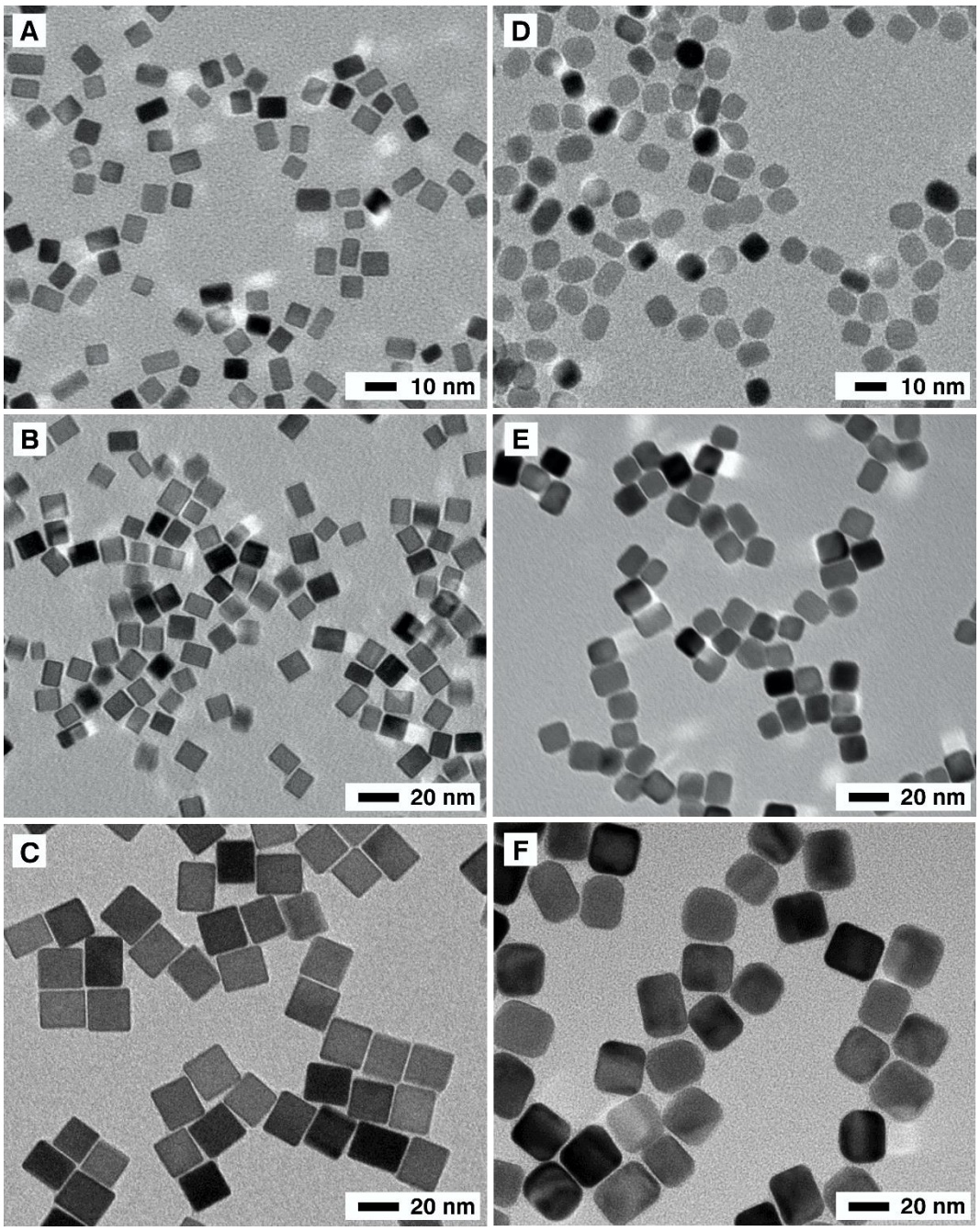

Fig. S14. TEM images of the Pd cubes of (*A*) 7, (*B*) 12, and (*C*) 23 nm in size that were used as the seeds and (*D-F*) the corresponding truncated cubes grown from these seeds when $PdBr_4^{2-}$ was added as a precursor.

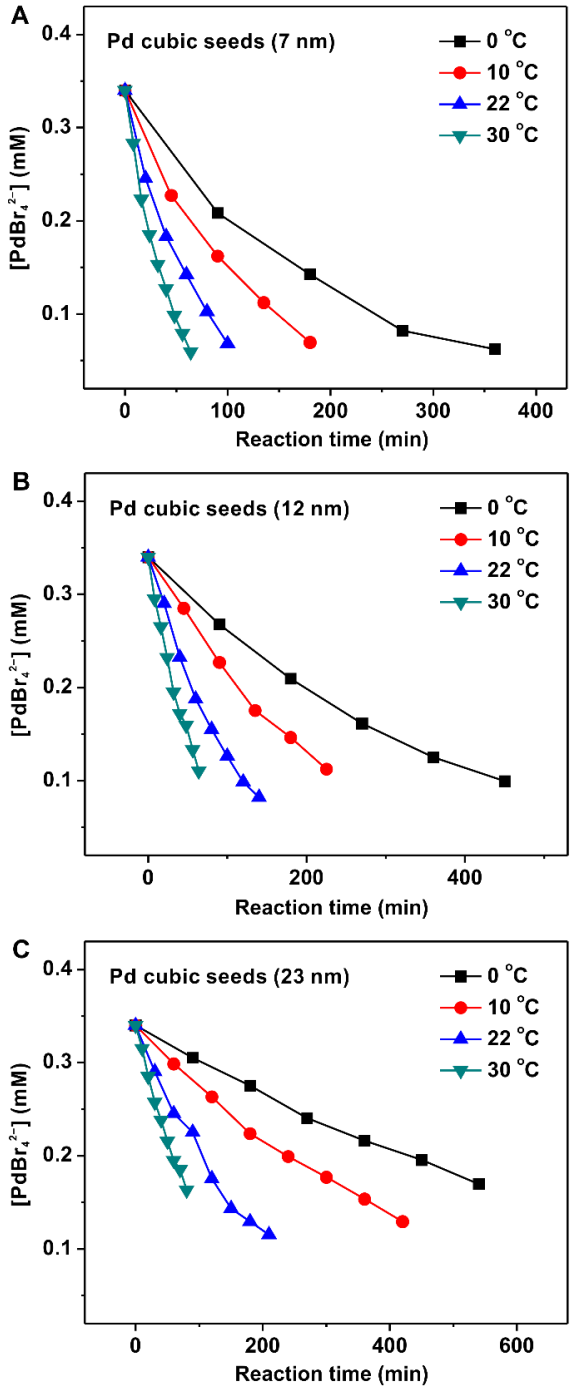

Fig. S15. Plots showing the concentrations of the Pd(II) precursor remaining in the reaction solutions as a function of time at different reaction temperatures when differently sized Pd cubic seeds were used: (*A*) 7, (*B*) 12, and (*C*) 23 nm.

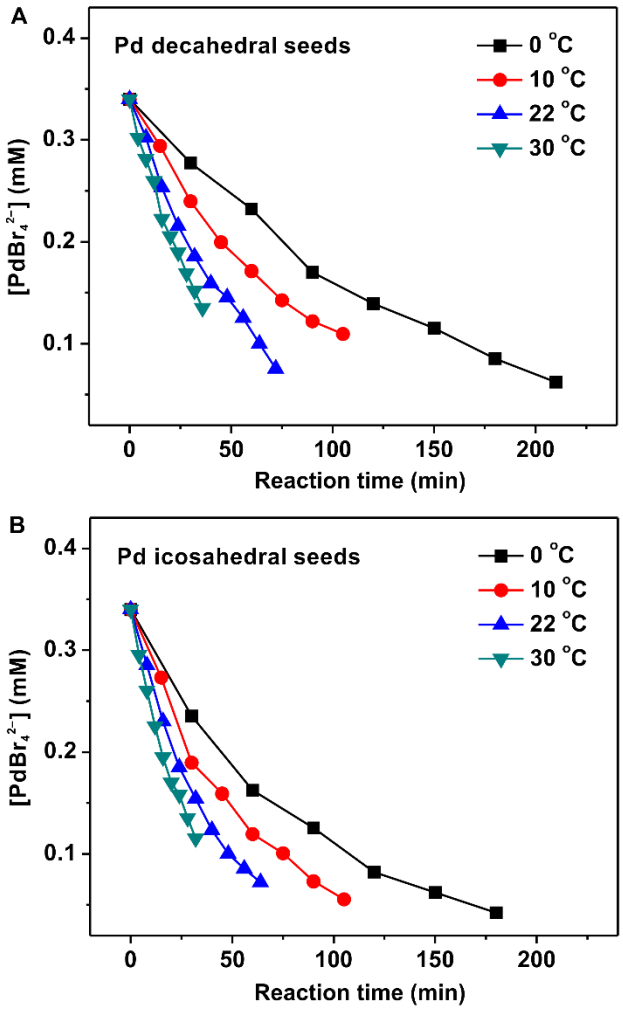

Fig. S16. Plots showing the concentrations of the Pd(II) precursor remaining in the reaction solutions as a function of time at different reaction temperatures when Pd (*A*) decahedral or (*B*) icosahedral seeds were involved, respectively.

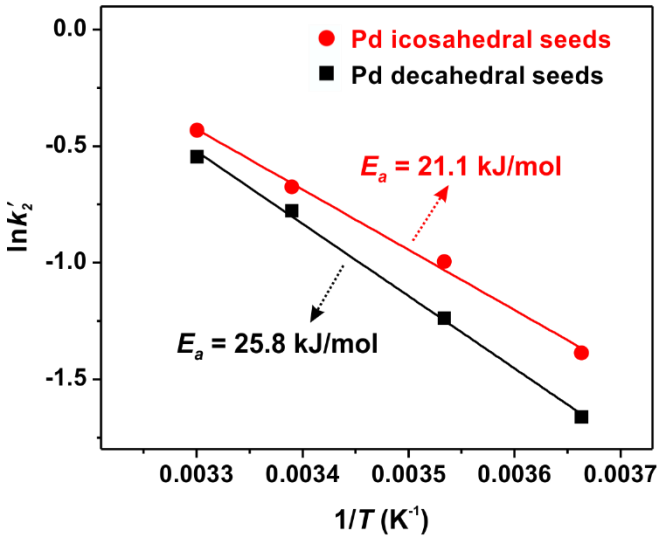

Fig. S17. A plot showing $\ln k_2'$ as a function of $1/T$ for the Pd(II) precursor in the presence of Pd decahedral and icosahedral seeds, respectively, where the slope of the linear regression line can be used to calculate the corresponding activation energy (E_a) for the autocatalytic surface reduction using the Arrhenius equation.

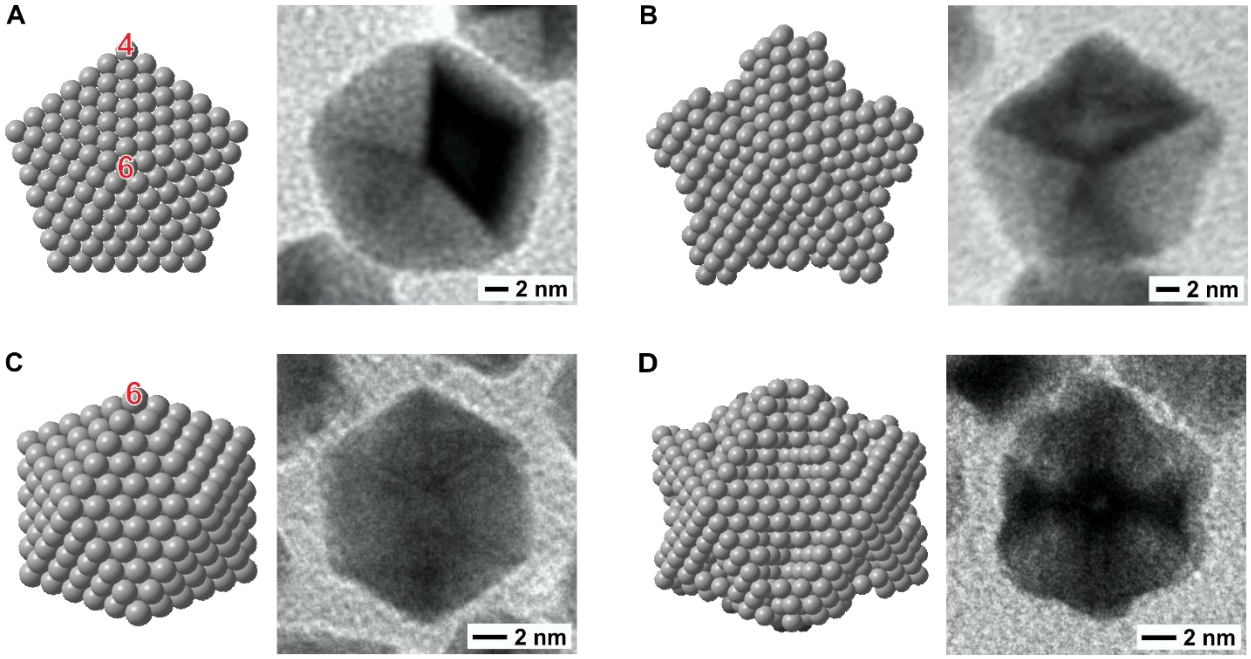

Fig. S18. (*A*, *C*) TEM images and the corresponding three-dimensional (3D) atomic models of individual Pd (*A*) decahedral and (*C*) icosahedral seeds. The numbers labeled on the atomic model are the coordination numbers of vertex atoms for a decahedron or icosahedron.[12] (*B*, *D*) TEM images and the corresponding 3D atomic models of individual (*B*) decahedral and (*D*) icosahedral nanocrystals obtained at $t = 0.5$ h from a standard synthesis when the Pd decahedral and icosahedral seeds were used. As opposed to the uniform deposition of Pd atoms on the entire decahedral and icosahedral surfaces, the growth of Pd preferentially took place from the low-coordination vertex sites located at the twin boundaries, resulting in the formation of Pd concave decahedra and icosahedra.

References

1. Peng HC, Park J, Zhang L, Xia Y (2015) Toward a quantitative understanding of symmetry reduction involved in the seed-mediated growth of Pd nanocrystals. *J Am Chem Soc* 137(20): 6643-6652.
2. Yang TH, et al. (2017) Toward a quantitative understanding of the reduction pathways of a salt precursor in the synthesis of metal nanocrystals. *Nano Lett* 17(1): 334-340.
3. Jin M, et al. (2011) Synthesis of Pd nanocrystals enclosed by {100} facets and with sizes <10 nm for application in CO oxidation. *Nano Res* 4(1): 83-91.
4. Peng HC, Xie S, Park J, Xia X, Xia Y (2013) Quantitative analysis of the coverage density of Br^- ions on Pd{100}facets and its role in controlling the shape of Pd nanocrystals. *J Am Chem Soc* 135(10): 3780-3783.
5. Jin M, Zhang H, Xie Z, Xia Y (2012) Palladium nanocrystals enclosed by {100} and {111} facets in controlled proportions and their catalytic activities for formic acid oxidation. *Energy Environ Sci* 5(4):6352-6357.
6. Huang H, et al. (2014) Polyol syntheses of palladium decahedra and icosahedra as pure samples by maneuvering the reaction kinetics with additives. *ACS Nano* 8(7): 7041-7050.
7. Wang X, et al. (2015) Palladium-platinum core-shell icosahedra with substantially enhanced activity and durability towards oxygen reduction. *Nat Commun* 6: 7594.
8. Watzky F, Finke RG (1997) Transition metal nanocluster formation kinetic and mechanistic studies. A new mechanism when hydrogen is the reductant: slow, continuous nucleation and fast autocatalytic surface growth. *J Am Chem Soc* 119(43): 10382-10400.
9. Lim B, et al. (2009) Shape-controlled synthesis of Pd nanocrystals in aqueous solutions. *Adv Funct Mater* 19(2): 189-200.

10. Van Hardeveld R, Hartog F (1969) The statistics of surface atoms and surface sites on metal crystals. *Surf Sci* 15(2):189-230.
11. Crespo-Quesada M, Yarulin A, Jin M, Xia Y, Kiwi-Minsker L (2011) Structure sensitivity of alkynol hydrogenation on shape- and size-controlled palladium nanocrystals: Which sites are most active and selective? *J Am Chem Soc* 133(32): 12787-12794.
12. Deng L, Deng H, Xiao S, Tang J, Hu W (2013) Morphology, dimension, and composition dependence of thermodynamically preferred atomic arrangements in Ag-Pt nanoalloys. *Faraday Discuss* 162: 293-306.